

hep-ph/9510449  
 CERN-TH/95-266  
 Edinburgh 95/556  
 GeF-TH-9/95

**NEXT-TO-LEADING ORDER DETERMINATION OF THE SINGLET AXIAL  
 CHARGE AND THE POLARIZED GLUON CONTENT OF THE NUCLEON**

Richard D. Ball†

*Theory Division, CERN,  
 CH-1211 Genève 23, Switzerland.*

and

*Department of Physics and Astronomy  
 University of Edinburgh, Edinburgh EH9 3JZ, Scotland*

Stefano Forte‡

*Theory Division, CERN,  
 CH-1211 Genève 23, Switzerland.*

Giovanni Ridolfi

*INFN, Sezione di Genova  
 Via Dodecaneso 33, I-16146, Genova, Italy*

**Abstract**

We perform a full next-to-leading analysis of the the available experimental data on the polarized structure function  $g_1$  of the nucleon, and give a precise determination of its singlet axial charge together with a thorough assessment of the theoretical uncertainties. We find that the data are now sufficient to separately determine first moments of the polarized quark and gluon distributions, and show in particular that the gluon contribution is large and positive.

Submitted to: *Physics Letters B*

CERN-TH/95-266  
 October 1995

---

† Supported in part by a Royal Society University Research Fellowship.

‡ On leave from INFN, Sezione di Torino, via P. Giuria 1, I-10125 Turin, Italy (address after December 1, 1995).

The polarized structure function  $g_1(x, Q^2)$  of the nucleon has been recently measured with good accuracy for proton [1] and deuteron [2] targets over a reasonably wide range of values of  $x$ . This opens up the possibility of a precise determination of the first moments of  $g_1$ , which are of direct physical interest, being related to the nucleon matrix elements of axial currents. An extraction of the moments of  $g_1$  from the data, however, requires theoretical input, not only because the data cover a limited range in  $x$  but, more importantly, because data are obtained at different values of  $Q^2$  for each  $x$  bin, and have thus to be evolved to a common value of  $Q^2$  using the Altarelli-Parisi equations before the moments can be evaluated (for recent reviews on the phenomenology of polarized structure functions see ref. [3]). We have recently shown [4] that these perturbative evolution effects can actually be quite large and substantially affect the extraction of the moments from  $g_1$ . Furthermore, effects which are formally next-to-leading order (NLO) may lead to significant evolution because of the large contribution of the polarized gluons to  $g_1$  driven by the axial anomaly.

The recent computation of the full matrix of two-loop anomalous dimensions [5] makes a consistent NLO analysis of  $g_1$  now possible. It is the purpose of this paper to perform such an analysis, and use it to provide a precise determination of the first moment of  $g_1$ . After reviewing the NLO formalism, discussing scheme dependence, and the effect of NLO corrections on the LO small- $x$  behaviour of parton distributions, we will use it to extract polarized parton distributions from the data. We will find that the data allow a determination of both the quark and gluon distributions without the need for extra theoretical assumptions, and in particular strongly constrain their overall normalizations and small- $x$  behaviours: we will thus be able to infer the existence of polarized gluons in the nucleon from an analysis of the scale dependence of  $g_1$ . We will then use these parton distributions to determine the first moment of the structure function  $g_1$  and the nucleon matrix element of the singlet axial current, or singlet axial charge, whose unexpected smallness has attracted a good deal of interest. We will finally provide an evaluation of the various sources of statistical and systematic error related to these determinations.

The structure function  $g_1$  is related to the polarized quark and gluon distributions by

$$g_1(x, Q^2) = \frac{\langle e^2 \rangle}{2} [C_{\text{NS}} \otimes \Delta q_{\text{NS}} + C_{\text{S}} \otimes \Delta \Sigma + 2n_f C_g \otimes \Delta g], \quad (1)$$

where  $\langle e^2 \rangle = \frac{1}{n_f} \sum_{i=1}^n e_i^2$ ,  $\otimes$  denotes the usual convolution with respect to  $x$ , the nonsinglet and singlet quark distributions are defined as

$$\Delta q_{\text{NS}} = \sum_{i=1}^{n_f} \left( \frac{e_i^2}{\langle e^2 \rangle} - 1 \right) (\Delta q_i + \Delta \bar{q}_i), \quad \Delta \Sigma = \sum_{i=1}^{n_f} (\Delta q_i + \Delta \bar{q}_i), \quad (2)$$

where  $\Delta q_i$  and  $\Delta \bar{q}_i$  are the polarized quark and antiquark distributions of flavor  $i$ , and  $\Delta g$  is the polarized gluon distribution (see ref. [4] for further details of notations and conventions.). The polarized parton distributions evolve according to the Altarelli-Parisi equations [6]

$$\begin{aligned} \frac{d}{dt} \Delta q_{\text{NS}} &= \frac{\alpha_s(t)}{2\pi} P_{qq}^{\text{NS}} \otimes \Delta q_{\text{NS}} \\ \frac{d}{dt} \begin{pmatrix} \Delta \Sigma \\ \Delta g \end{pmatrix} &= \frac{\alpha_s(t)}{2\pi} \begin{pmatrix} P_{qq}^{\text{S}} & 2n_f P_{qg}^{\text{S}} \\ P_{gq}^{\text{S}} & P_{gg}^{\text{S}} \end{pmatrix} \otimes \begin{pmatrix} \Delta \Sigma \\ \Delta g \end{pmatrix}, \end{aligned} \quad (3)$$

where  $t \equiv \ln(Q^2/\Lambda^2)$ . The coefficient functions  $C$  and splitting functions  $P$  may each be expanded in powers of  $\alpha_s$ : at NLO

$$C(x, \alpha_s) = C^{(0)}(x) + \frac{\alpha_s}{2\pi} C^{(1)}(x) + O(\alpha_s^2) \quad (4)$$

$$P(x, \alpha_s) = P^{(0)}(x) + \frac{\alpha_s}{2\pi} P^{(1)}(x) + O(\alpha_s^2). \quad (5)$$

In accordance with the partonic picture  $C_{\text{NS}}^{(0)}(x) = C_S^{(0)}(x) = \delta(1-x)$ , while  $C_g^{(0)}(x) = 0$ . It will also prove convenient to introduce anomalous dimensions  $\gamma(N, \alpha_s) \equiv \int_0^1 dx x^{N-1} P(x, \alpha_s)$ , i.e. the Mellin transforms of the splitting functions, as well as analogously defined moment-space coefficient functions  $C(N, \alpha_s)$  and parton distributions  $\Delta q_{\text{NS}}(N, Q^2)$ ,  $\Delta \Sigma(N, Q^2)$  and  $\Delta g(N, Q^2)$ .

Whereas the NLO coefficient functions  $C^{(1)}$  have been known for some time [7] the two loop splitting functions  $P^{(1)}$  have been only recently determined [5],<sup>1</sup> only their first moments being known previously [7]. The NLO coefficient functions may be modified by a change of factorization scheme which is partially compensated by a corresponding change in the NLO anomalous dimensions, hence both are required in order to specify a NLO computation completely. Previous analyses which included NLO effects only in the coefficient functions (such as [4]) were thus necessarily incomplete and treated only the first moments consistently at NLO. It is now possible to test explicitly whether, as was claimed in ref. [4], the NLO gluon contribution to the first moment of  $g_1$  is the dominant NLO effect, and furthermore whether it has a sizable effect on the  $Q^2$  dependence of  $g_1$ .

The NLO anomalous dimensions and coefficient functions of ref. [5] are given in the  $\overline{\text{MS}}$  scheme. Since chiral symmetry is respected, matrix elements of nonsinglet axial currents are conserved, nonsinglet axial charges do not evolve, and thus  $\Delta q_{\text{NS}}(1, Q^2)$  is independent of  $Q^2$ . In all such schemes at NLO

$$C_{\text{NS}}(1, \alpha_s) = C_S(1, \alpha_s) = 1 - \frac{\alpha_s}{\pi} + O(\alpha_s^2) \quad (6)$$

(although at higher orders  $C_{\text{NS}}(1, \alpha_s) \neq C_S(1, \alpha_s)$ ). Matrix elements of the axial singlet current are instead not conserved because of the axial anomaly, so that the singlet axial charge depends on scale. In the  $\overline{\text{MS}}$  scheme the first moment of  $C_g^{(1)}$  vanishes, the gluon decouples from the first moment of  $g_1$  and the scale dependent singlet axial charge is thus equal to  $\Delta \Sigma(1, Q^2)$ .

Factorization schemes where this happens are somewhat pathological, in that they include soft contributions to the cross section in the coefficient function rather than absorbing them completely into the parton distributions [8-10]. We will instead perform our calculations in schemes where all soft contributions are properly factorized into the parton distributions. The first moment of the gluon coefficient function at NLO is then [11]

$$C_g(1, \alpha_s) = -\frac{\alpha_s}{4\pi} + O(\alpha_s^2). \quad (7)$$

---

<sup>1</sup> With our conventions the expressions of  $\gamma^{(0)}$  and  $\gamma^{(1)}$  of ref. [5] must be divided by  $-4$  and  $-8$  respectively and  $\gamma_{qg}$  should be further divided by  $2n_f$ .

With this choice, the first moment of  $g_1$  is given at NLO by

$$\Gamma_1(Q^2) \equiv \int_0^1 g_1(x, Q^2) dx = \frac{\langle e^2 \rangle}{2} \left[ \left(1 - \frac{\alpha_s}{\pi}\right) (\Delta q_{\text{NS}}(1, Q^2) + \Delta \Sigma(1, Q^2)) - n_f \frac{\alpha_s}{2\pi} \Delta g(1, Q^2) \right], \quad (8)$$

and the first moment of the scale dependent eigenvector of the singlet Altarelli-Parisi equations (3) is

$$a_0(Q^2) = \Delta \Sigma(1, Q^2) - n_f \frac{\alpha_s}{2\pi} \Delta g(1, Q^2). \quad (9)$$

The corresponding eigenvalue of the anomalous dimension matrix coincides with the anomalous dimension of the singlet axial current, so  $a_0$  is identified with the singlet axial charge

$$\langle p, s | j_5^\mu | p, s \rangle = M s^\mu a_0(Q^2), \quad (10)$$

where  $p$ ,  $M$  and  $s$  are the momentum, mass and spin of the nucleon. The other eigenvector of perturbative evolution is the first moment of the polarized singlet quark distribution,  $\Delta \Sigma(1, Q^2)$ , which is then independent of  $Q^2$ , and may be identified with the conserved singlet quark helicity [11-13].

In fact the eigenvectors remain the same to all orders in perturbation theory, because of the Adler-Bardeen theorem [14], which states that the NLO mixing of the divergence of the singlet axial current with a gluonic operator (the anomaly), which is responsible for its scale dependence, does not receive higher order corrections. Thus if we require that  $\Delta \Sigma(1, Q^2)$  is scale independent then the axial charge is given by eq. (9) to all orders. This means that the first moments of the singlet quark and gluon coefficient functions are not actually independent: to all orders in perturbation theory (8) becomes simply

$$\Gamma_1(Q^2) = \frac{\langle e^2 \rangle}{2} \left[ C_{\text{NS}}(1, \alpha_s) \Delta q_{\text{NS}}(1, Q^2) + C_{\text{S}}(1, \alpha_s) a_0(Q^2) \right], \quad (11)$$

and thus

$$C_g(1, \alpha_s) = -\frac{\alpha_s}{4\pi} C_{\text{S}}(1, \alpha_s). \quad (12)$$

Given anomalous dimensions and coefficient functions in a particular factorization scheme any other factorization scheme can be constructed [15] by introducing a scheme change specified by a function  $z_{\text{NS}}(N, \alpha_s) = 1 + \frac{\alpha_s}{2\pi} z_{\text{NS}}^{(1)}(N) + O(\alpha_s^2)$  and a matrix  $z_{\text{S}}(N, \alpha_s) = \mathbb{1} + \frac{\alpha_s}{2\pi} z_{\text{S}}^{(1)}(N) + O(\alpha_s^2)$ . The NLO anomalous dimensions and coefficient functions then change according to

$$\begin{aligned} \gamma_{\text{NS}}^{(1)}(N) &\rightarrow \gamma_{\text{NS}}^{(1)}(N) - \frac{\beta_0}{2} z_{\text{NS}}^{(1)}(N), \\ \gamma_{\text{S}}^{(1)}(N) &\rightarrow \gamma_{\text{S}}^{(1)}(N) + [z_{\text{S}}^{(1)}(N), \gamma_{\text{S}}^{(0)}(N)] - \frac{\beta_0}{2} z_{\text{S}}^{(1)}(N), \end{aligned} \quad (13)$$

$$\begin{aligned} C_{\text{NS}}^{(1)}(N) &\rightarrow C_{\text{NS}}^{(1)}(N) - z_{\text{NS}}^{(1)}(N), \\ C_{\text{S}}^{(1)}(N) &\rightarrow C_{\text{S}}^{(1)}(N) - z_{qq}^{(1)}(N), \\ C_g^{(1)}(N) &\rightarrow C_g^{(1)}(N) - z_{gg}^{(1)}(N), \end{aligned} \quad (14)$$

where  $\beta_0 = 11 - \frac{2}{3}n_f$  is the one loop coefficient of the QCD beta function.

For simplicity we will only discuss scheme changes where  $z_{\text{NS}} = z_{qq}$ , i.e. such that the relative normalization of the singlet and nonsinglet quark distributions is unaffected. The conservation of the nonsinglet axial current then fixes the first moment  $z_{\text{NS}}^{(1)} = z_{qq}^{(1)} = 0$  whenever the original scheme respects chiral symmetry. We then wish to consider specifically factorization schemes in which the first moments of the coefficient functions satisfy eq. (7): starting from the  $\overline{\text{MS}}$  scheme, eq. (14) then fixes  $z_{qg}^{(1)}(1) = 1$ .<sup>2</sup> In order to completely specify the first moment of  $z$  we use the Adler-Bardeen condition that the two-loop eigenvector of perturbative evolution as given by (9) be identified to all perturbative orders with the matrix element of the axial current. Knowledge of the NNLO anomalous dimension of the axial current [17] then fixes the first moments of the remaining two entries of the matrix  $z$ .

We will consider several schemes which differ in the way the remaining moments of the coefficient functions and anomalous dimensions are constructed. In the first scheme, we simply take  $z(x)$ , the inverse Mellin transform of  $z(N)$ , to be independent of  $x$ . This scheme is thus the minimal modification of the  $\overline{\text{MS}}$  scheme such that the first moments of parton distributions satisfy the anomaly constraint eq. (9); in particular, the large and small  $x$  behaviour of the coefficient functions and anomalous dimensions are then the same as in  $\overline{\text{MS}}$ . We will refer to this as the Adler-Bardeen (AB) scheme. The matrix which transforms from  $\overline{\text{MS}}$  to the AB scheme is

$$z_{\text{S}}^{(1)}(N)|_{\text{AB}} = \frac{1}{N} \begin{pmatrix} 0 & 2n_f T_F \\ 0 & 0 \end{pmatrix}, \quad (15)$$

where, for SU(3) color,  $C_F = \frac{4}{3}$ ,  $C_A = 3$  and  $T_F = \frac{1}{2}$ . Notice that the two lower entries in the  $\overline{\text{MS}}$  NLO anomalous dimension matrix [5] turn out to be already consistent with the Adler-Bardeen condition above, and NNLO anomalous dimensions [17]; the corresponding entries of the scheme change matrix eq. (15) therefore vanish.

Transformations such as (15) which take us from  $\overline{\text{MS}}$  to a scheme where the gluon contributes to the first moment of  $g_1$  correspond to removing soft contributions from the coefficient functions [9-10]. Rather than doing this by hand, as in the AB scheme above, the subtraction may be performed by computing the coefficient functions in the presence of an explicit infrared regulator, which automatically enforces eq. (7) [10]. The entries  $z_{qq}$  and  $z_{qg}$  of the  $z$  matrix are then fixed using eq. (14) and the  $\overline{\text{MS}}$  coefficient functions [5]

$$\begin{aligned} C_q^{\text{S}^{(1)}}(N)|_{\overline{\text{MS}}} &= C_F \left[ S_1(N) \left( \frac{3}{2} - \frac{1}{N(N+1)} + S_1(N) \right) - S_2(N) - \frac{9N^3 + 6N^2 - 3N - 2}{2N^2(N+1)} \right], \\ C_g^{\text{S}^{(1)}}(N)|_{\overline{\text{MS}}} &= -T_F \frac{N-1}{N(N+1)} \left( S_1(N) + \frac{N-1}{N} \right), \end{aligned} \quad (16)$$

where  $S_j(N) = \sum_{k=1}^N \frac{1}{k^j}$ . The two lower entries of the transformation matrix can then be taken to be zero as in the AB scheme.

---

<sup>2</sup> A scheme change of this kind was constructed in ref. [16]; the form of the matrix  $z$  given there appears however to be incorrect. Also, note that the partial result for the NLO splitting functions given there is incorrect, as explained in ref. [5].

One possibility is to renormalize while keeping the incoming particle off-shell (OS scheme, henceforth); the coefficient functions are then given by

$$\begin{aligned} C_q^{\text{S}(1)}(N)|_{\text{OS}} &= C_F \left( \frac{3}{2} S_1(N) - 4S_2(N) - \frac{2N^4 - N^3 - 5N - 4}{2N^2(N+1)^2} \right), \\ C_g^{\text{S}(1)}(N)|_{\text{OS}} &= -2T_F \frac{N^3 - N^2 + N + 1}{N^2(N+1)^2}. \end{aligned} \quad (17)$$

An alternative option is to endow the quarks with a finite mass (Altarelli-Ross, or AR scheme); the quark [18]<sup>3</sup> and gluon [11,10] coefficient functions are then

$$\begin{aligned} C_q^{\text{S}(1)}(N)|_{\text{AR}} &= C_F \left[ \left( \frac{7}{2} + \frac{1}{N(N+1)} - S_1(N) \right) S_1(N) - 3S_2(N) - \frac{5N^4 + 7N^3 + 5N^2 - 3N - 2}{2N^2(N+1)^2} \right], \\ C_g^{\text{S}(1)}(N)|_{\text{AR}} &= -T_F \frac{N^2 + 1 + N(N-1)S_1(N)}{N^2(N+1)}. \end{aligned} \quad (18)$$

Notice that in all three of these schemes the first moments of the coefficient functions are given by eqs. (6) and (7), and thus the NLO relation between the first moment of  $g_1$  and the singlet axial charge  $a_0$  implicit in eqs. (8) and (9) is automatically satisfied.

The main effect of the NLO corrections to perturbative evolution is the coupling of the gluon to  $g_1$ , and in particular its contribution to the first moment  $\Gamma_1$  eq. (8), which does not decouple as  $Q^2 \rightarrow \infty$  [11]. However, NLO corrections may also substantially affect the small- $x$  behaviour of parton distributions and coefficient functions. Indeed, unlike the unpolarized case, the NLO contributions to the polarized splitting functions and coefficient functions display a stronger singularity as  $x \rightarrow 0$  than their LO counterparts; accordingly their Mellin transforms display a stronger singularity as  $N \rightarrow 0$ . More specifically the singularities in the NLO  $\overline{\text{MS}}$  anomalous dimensions [5] and coefficient functions take the form

$$\begin{aligned} \gamma_{\text{NS}}^{(1)}(N) &= \frac{1}{N^3} (2C_A C_F - 3C_F^2) + O\left(\frac{1}{N^2}\right), \\ \gamma_{\text{S}}^{(1)}(N) &= \frac{1}{N^3} \begin{pmatrix} -4C_F T_F n_f + 2C_A C_F - 3C_F^2 & -2C_A T_F - C_F T_F \\ 4C_A C_F + 2C_F^2 & 8C_A^2 - 4C_F T_F n_f \end{pmatrix} + O\left(\frac{1}{N^2}\right), \\ C_{\text{NS}}^{(1)} = C_q^{(1)} &= C_F \frac{1}{N^2} + O\left(\frac{1}{N}\right), \quad C_g^{(1)} = -T_F \frac{1}{N^2} + O\left(\frac{1}{N}\right), \end{aligned} \quad (19)$$

whereas the LO anomalous dimensions have a simple pole in  $N$  (details of which may be found in ref. [4]).<sup>4</sup>

---

<sup>3</sup> Because the quark mass breaks chiral symmetry, it is now necessary to perform an extra subtraction in order to ensure that the nonsinglet axial currents are conserved.

<sup>4</sup> The presence of double logarithms in the NLO polarized splitting functions and coefficient functions strongly suggests that the systematic cancellation of collinear singularities which characterizes the small- $x$  behaviour of unpolarized splitting functions does not occur in the polarized case. In the nonsinglet channel a summation of these double logarithmic singularities to all orders in  $\alpha_s$  has been attempted in ref. [19].

The NLO corrections could therefore have a significant impact in the small  $x$  region, and in particular require a summation of logarithmic effects in  $\frac{1}{x}$ , which could be done in analogy to the unpolarized case [20] if the coefficient of the most singular contributions to the polarized splitting functions as  $x \rightarrow 0$  were known to all orders in  $\alpha_s$ . In order to assess at which values of  $x$  and  $Q^2$  these effects might begin to be relevant (and in particular whether they already amount to a sizable correction in the presently measured region)  $g_1$  may be determined by solving the NLO evolution equations with the approximate small- $N$  form eq. (19) of the anomalous dimensions:

$$\begin{aligned}\Delta q_{\text{NS}}(N, Q^2) &= \Delta q_{\text{NS}}(N, Q_0^2) \left( \frac{\alpha_s(Q_0^2)}{\alpha_s(Q^2)} \right)^{\frac{2\gamma_{\text{NS}}^{(0)}(N)}{\beta_0}} \left[ 1 + \frac{\epsilon_{\text{NS}}}{N^3} (\alpha_s(Q_0^2) - \alpha_s(Q^2)) \right], \\ v_{\pm}(N, Q^2) &= v_{\pm}(N, Q_0^2) \left( \frac{\alpha_s(Q_0^2)}{\alpha_s(Q^2)} \right)^{\frac{2\lambda_{\pm}(N)}{\beta_0}} \left[ 1 + \frac{\epsilon_{\pm}}{N^3} (\alpha_s(Q_0^2) - \alpha_s(Q^2)) \right],\end{aligned}\tag{21}$$

where  $v_{\pm}$  and  $\lambda_{\pm}$  are the eigenvectors and eigenvalues of the LO singlet anomalous dimension matrix  $\gamma^{(0)}$  (see ref. [4]),  $\alpha_s(Q^2)$  is computed at NLO,  $Q_0$  is the starting scale, and the coefficients  $\epsilon$  are explicitly given by

$$\epsilon_{\text{NS}} = \frac{8}{3\pi\beta_0}, \quad \epsilon_{\pm} = \frac{112}{3\pi\beta_0} \left[ \left( 1 - \frac{n_f}{14} \right) \pm \frac{13}{14} \left( 1 - \frac{11n_f}{104} \right) / \sqrt{1 - \frac{3n_f}{32}} \right].\tag{22}$$

The NLO corrections do not mix the LO small  $x$  eigenvectors, because mixing terms are  $O(\frac{1}{N^2})$ . The eigenvectors of perturbative evolution at NLO are thus the same as at LO: at small  $x$  and large  $Q^2$   $\Delta g$  and  $\Delta\Sigma$  have opposite sign [4], and in particular (for any plausible parton distributions)  $\Delta\Sigma < 0$  and  $\Delta g > 0$ . It is interesting to observe that this result is scheme independent, because the leading  $\frac{1}{N^3}$  singularities in the NLO corrections only receive contributions from the diagonal projections of the NLO anomalous dimension matrix onto the LO eigenvectors, which are themselves scheme independent.

The leading NLO small- $x$  behaviour can now be found by inverse Mellin transform of eq. (21) in the saddle point approximation:

$$\begin{aligned}\Delta q_{\text{NS}}(x, Q^2) &= \mathcal{N}_{\text{NS}} \sigma^{-1/2} e^{2\gamma_{\text{NS}}\sigma} \left[ 1 + \epsilon_{\text{NS}} \left( \frac{\rho}{\gamma_{\text{NS}}} \right)^3 (\alpha_s(Q_0^2) - \alpha_s(Q^2)) \right], \\ v_{\pm}(x, Q^2) &= \mathcal{N}_{\pm} \sigma^{-1/2} e^{2\gamma_{\pm}\sigma} \left[ 1 + \epsilon_{\pm} \left( \frac{\rho}{\gamma_{\pm}} \right)^3 (\alpha_s(Q_0^2) - \alpha_s(Q^2)) \right],\end{aligned}\tag{23}$$

where  $\mathcal{N}$  are normalization constants,  $\sigma \equiv \sqrt{\xi\zeta}$ ,  $\rho \equiv \sqrt{\xi/\zeta}$ ,  $\xi \equiv \ln \frac{x_0}{x}$ ,  $\zeta \equiv \ln \frac{\alpha_s(Q_0^2)}{\alpha_s(Q^2)}$ ,  $x_0$  is a reference value of  $x$  such that the approximate small- $x$  form of the anomalous dimensions is applicable for  $x \lesssim x_0$  and  $Q^2 \gtrsim Q_0^2$ , and  $\gamma_{\text{NS}}^2 = \frac{2C_F}{\beta_0}$  while  $\gamma_{\pm}$  are as given in ref. [4].<sup>5</sup>

---

<sup>5</sup> Eq. (23) only gives the NLO generalization of the asymptotic LO behaviour  $\sigma^{-1/2} e^{2\gamma\sigma}$  when the boundary conditions are soft, as discussed in ref. [4]. If the boundary condition is hard, for example  $e^{\xi\lambda}$ , then for  $\rho \gtrsim \gamma/\lambda$  the LO behaviour reproduces the boundary condition [4], and the NLO correction to it is given by  $[1 + \epsilon_i \lambda^{-3} (\alpha_s(Q_0^2) - \alpha_s(Q^2))]$ , where  $\epsilon_i = \epsilon_{\text{NS}}, \epsilon_{\pm}$  in the nonsinglet and singlet cases respectively. In this case the NLO correction is thus  $x$ -independent.

The terms in square brackets in eq. (23) give the NLO correction to the LO asymptotic small  $x$  behaviour [4,21]. Because all coefficients  $\epsilon$  eq. (22) are positive the NLO corrections lead to a further increase proportional to  $\xi^{3/2}$  of the parton distributions at small  $x$ . The coefficient of this increase is however rather small, for instance with  $n_f = 4$  one gets  $\epsilon_{\text{NS}}/\gamma_{\text{NS}}^3 \approx \epsilon_+/\gamma_+^3 \approx \frac{1}{2}$ , so that the correction is small in the presently accessible small  $x$  region. These conclusions however only apply to the region where the no summation of logs of  $\frac{1}{x}$  is necessary so that the NLO in  $\alpha_s$  may be treated as a subleading correction, and could be substantially altered at smaller values of  $x$ .

The leading small  $x$  behaviour of  $g_1$  can be found at NLO using the small  $x$  NLO solution eq. (21) and coefficient functions eq. (20) in the Mellin transform of the expression of  $g_1$  eq. (1). Because the NLO coefficient functions (20) only have a  $\frac{1}{N^2}$  singularity at NLO they actually do not contribute to the leading small- $x$  behaviour of  $g_1$ , which is thus found by simply taking the appropriate linear combination of the small- $x$  parton distributions eq. (23). The NLO correction to the small- $x$  behaviour of the coefficient functions may nevertheless have a significant impact, especially at low scales (i.e., when  $Q$  is close to the starting scale  $Q_0$ ) where evolution effects are negligible. Indeed, the  $\frac{1}{N^2}$  singularity corresponds to a  $\log \frac{1}{x}$  rise of the coefficient function, and would therefore lead to a rise of both singlet and nonsinglet contributions to the structure function  $g_1$  even if the parton distributions themselves did not rise. The coefficient of this rise is however not scheme independent: for instance, the coefficient of the leading singularity in the gluon coefficient function is the same in the  $\overline{\text{MS}}$ , AB and AR schemes, but is twice as large in the OS scheme.

Having established that a NLO treatment is adequate in the region of current experimental data, we can proceed to a determination of the physical observables related to  $g_1$ . Even though our purpose here is not to establish a parametrization of polarized parton distributions, we have to construct such a parametrization since only LO parametrizations are currently available<sup>6</sup>. We parametrize the initial parton distributions according to

$$\Delta f(x, Q_0^2) = N(\alpha_f, \beta_f, a_f) \eta_f x^{\alpha_f} (1-x)^{\beta_f} (1+a_f x), \quad (24)$$

where  $N(\alpha, \beta, a)$  is fixed by the normalization condition  $N(\alpha, \beta, a) \int_0^1 dx x^\alpha (1-x)^\beta (1+ax) = 1$ , and  $\Delta f$  denotes  $\Delta\Sigma$ ,  $\Delta q_{\text{NS}}$  or  $\Delta g$ . In our previous analysis [4], which used only proton data, the respective three sets of parameters could not be independently determined, while the small  $x$  behaviour had to be fixed and then varied in a plausible range. Now, by including the deuteron data [2], we can disentangle the nonsinglet and singlet quark and gluon contributions to  $g_1$ , because  $g_1^p$  is dominated by the isotriplet term, which contributes about 90% of its first moment, while  $g_1^d$  is isosinglet. We can thus determine independently almost all of the parameters of the singlet and nonsinglet parton distributions (including the parameters  $\alpha_f$ , which determine their small- $x$  behaviour).

We determine  $g_1$  at all  $x$  and  $Q^2$  by solution of the NLO evolution equations with boundary conditions of the form (24) at  $Q_0^2 = 1 \text{ GeV}^2$ . The various parameters in eq. (24)

---

<sup>6</sup> A comprehensive review of the present status of polarized parton parametrizations is given in ref. [22]. A NLO parametrization has been presented in ref. [23], but in the unsubtracted  $\overline{\text{MS}}$  scheme, which, as previously discussed, is not properly factorized.

are then found by fitting  $g_1(x, Q^2)$  to the recent precision experimental determination of  $g_1$  for proton and deuteron [1,2], which are given along a curve  $Q^2 = Q^2(x)$  for each experiment. As in [4]  $g_1$  is extracted from the measured asymmetry  $A_1$  using the leading-twist expression<sup>7</sup>  $g_1(x, Q^2) = A_1(x, Q^2)F_1(x, Q^2)$ ;  $F_1$  is in turn computed from the SLAC determination [24] of the ratio  $R(x, Q^2)$  of the longitudinal to transverse virtual photoabsorption cross section, and the most recent NMC determination [25] of  $F_2(x, Q^2)$ . The deuteron structure function is defined as the average of the proton and neutron structure functions and is obtained from the deuteron asymmetry after applying a correction to account for  $d$ -wave admixture [26]:

$$g_1^d(x, Q^2) \equiv \frac{1}{2}(g_1^p(x, Q^2) + g_1^n(x, Q^2)) = A_1^d(x, Q^2)F_1^d(x, Q^2)/(1 - 1.5\omega_D) \quad (25)$$

where  $\omega_D = 0.05$ .

The normalization of the nonsinglet quark distribution at  $Q_0$  (which lies below the charm threshold) is fixed by assuming SU(3) symmetry of the matrix elements of the axial current, determined [27] from hyperon  $\beta$  decays:

$$\eta_{\text{NS}} = \int_0^1 \Delta q_{\text{NS}}(x, Q^2) dx = \pm \frac{3}{4}g_A + \frac{1}{4}a_8, \quad (26)$$

$$g_A = 1.2573 \pm 0.0028; \quad a_8 = 0.579 \pm 0.025, \quad (27)$$

where the plus (minus) sign refers to a proton (neutron) target. While the impact of possible SU(3) violation on our results will be discussed below, we will defer to a subsequent publication the possibility of using the data themselves to test SU(3) or SU(2) (and thus the Bjorken sum rule). At higher scales, new nonsinglet contributions arise as the various heavy quark thresholds are passed, so that  $\Delta q_{\text{NS}}(1, Q^2)$  is not scale independent across thresholds. The corresponding heavy quark distributions are generated dynamically, assuming that they vanish on threshold, and imposing [9] continuity of  $a_0(Q^2)$  eq. (9).

It turns out that the data are good enough to determine all the remaining parameters directly with a single exception, namely, the parameters  $a_q$  and  $a_g$  which control the shape of the singlet distributions  $\Delta\Sigma$  and  $\Delta g$  at intermediate  $x$ , and which are difficult to pin down individually since the evolution mixes  $\Delta\Sigma$  and  $\Delta g$ . We will thus take  $a_q = a_g$ , and determine the remaining ten parameters from a fit to the data. The respective best fit values are listed, in table 1 for the AB, AR and OS schemes. The errors given there are statistical errors from the fit, computed by taking into account correlations. The corresponding determination of  $g_1(x)$  in the AB scheme is shown in fig. 1 at the starting scale as well as at the scale  $Q(x)$  of the various data sets and at  $Q^2 = 10 \text{ GeV}^2$ .

The main features of this determination of polarized parton distributions are the following. The evolution of  $g_1$  is rather similar to that discussed in ref. [4], thus demonstrating that the main NLO effect is indeed the direct gluon contribution to the first moment of  $g_1$  which was already included there; the main difference between the present determination

---

<sup>7</sup> Kinematic higher twist corrections which are sometimes included are neglected here for consistency since no systematic treatment of these corrections is available.

of polarized parton distributions and that of ref. [4] is the more detailed nature of the fit, due to the inclusion of the deuteron data.

Specifically, the large  $x$  behaviour, controlled by the exponent  $\beta$ , is in fair agreement with the expectations based on QCD counting rules [28], which predict  $\beta_q = \beta_{\text{NS}} \simeq 3$  and  $\beta_g \simeq 4$ ; of course these parameters are strongly scheme dependent (as explicitly displayed in table 1). The value of  $\beta_g$  cannot be determined very accurately since large- $x$  data are at relatively large  $Q^2$ , where the direct coupling of the gluon to  $g_1$  is suppressed by the small value of  $\alpha_s$ ; in the OS scheme the results are largely independent of this coefficient which thus cannot be fitted at all.

The small  $x$  behaviour turns out to be at least qualitatively constrained by the data. The initial singlet parton distributions are found to display soft valence-like behaviour, i.e. not to grow at small  $x$ , as was predicted by Regge theory [29]. However the nonsinglet quark distribution is found to grow approximately as  $\Delta q \underset{x \rightarrow 0}{\sim} \frac{1}{\sqrt{x}}$ .<sup>8</sup> We have explicitly verified that these behaviours indeed correspond to an overall global minimum, and that the quality of the fit deteriorates uniformly as the values of  $\alpha_f$  deviate from those given in table 1, by repeating the fit with fixed values of the three exponents  $\alpha_f$  chosen in the range  $-0.9 \leq \alpha_f \leq +0.5$ . The singular behaviour of the nonsinglet quark is the main difference between these results and those discussed in ref. [4], where, since it was impossible to determine it from the data, it was assumed to be valence-like.

Even though these results are suggestive, they should be taken with some care: firstly, the values of  $\alpha_f$  are strongly scheme-dependent, and partly just reflect the shape of the coefficient functions at small  $x$  and small  $Q^2$  in the various schemes: for instance, the fact that the coefficient of the leading singularity in  $C_g^{(1)}$  is larger in the OS scheme explains why the value of  $\alpha_g$  in this scheme is larger. Furthermore, these are not necessarily the asymptotic behaviours of the various parton distributions as  $x \rightarrow 0$ : in particular, the large value and uncertainty in  $a_{\text{NS}}$  indicate that the asymptotic behaviour of  $g_1^p$  is still setting in at the smallest experimental  $x$  values; likewise,  $g_1^d$  at small  $Q^2$  and small  $x$  grows large and positive with the present parametrization, but this happens outside the data range (the growth is barely seen starting on the  $Q^2 = 1 \text{ GeV}^2$  curve of Fig. 1b). In this respect, present-day polarized data are to be compared to the NMC unpolarized data [25]: a kinematic coverage comparable to that available at HERA for determining [31] the small- $x$  behaviour  $F_2$  would be required to determine precisely the small  $x$  behaviour of polarized parton distributions. This is reflected by the large uncertainties in the parameters  $a_f$  which govern the transition to the small  $x$  region.

Finally, the data turn out to allow a good determination of the size of the quark and gluon distributions. The size of the gluon distribution drives perturbative evolution; the evolution already observed due to the fact that the SMC and E143 data are taken at different values of  $Q^2$  for equal  $x$  (displayed in fig. 1) turns out to be sufficient to require  $\eta_g$  (which gives the first moment of  $\Delta g$  at the initial scale  $Q = Q_0$ ) to be large and positive. The relation eq. (9) between the first moments of the quark and gluon distributions and the first moment of  $g_1$  then inevitably leads to a rather large quark singlet. This is a remarkable

---

<sup>8</sup> This seems to be qualitatively consistent with the summation of double logarithms presented in refs.[19,30], since this suggests that both the polarized and unpolarized nonsinglet quark distributions have the same leading small  $x$  behaviour, at least in perturbation theory.

result: the scale-independent first moment of  $\Delta\Sigma$ , given by  $\eta_q$ , is found empirically to be equal to  $a_8$  eq. (27) within errors. The large violation of the Zweig rule in the first moment of  $g_1$  appears then to be almost entirely due to a large perturbative gluon contribution to  $g_1$ , as was conjectured in ref. [11].

A large gluon distribution implies substantial evolution effects, and thus a substantial correction due to the determination of the moments of  $g_1$  from the experimental data [4]. Indeed, we can now determine the first moment eq. (8), as well as the singlet axial charge of the nucleon defined according to eq. (9) from the best-fit polarized parton distributions. The results in the AB scheme, which we shall take as a baseline, are displayed in the first row of table 2. Only  $\Gamma_1^p$  is shown; the deuteron is obtained from it by subtracting the isotriplet contribution  $\Gamma_1^{I=1} = \frac{1}{12}C_{\text{NS}}(1, \alpha_s)g_A$  since we have assumed isospin to be exact. The value of  $\Gamma_1$  is found to be lower than the value extracted [1,2] neglecting the evolution of the asymmetry, and consequently the value of the axial charge  $a_0$  we obtain is about a half of the value quoted by the experimental collaborations. It is thus important to establish whether this result is a robust consequence of the inclusion of NLO evolution effects, or whether it is a by-product of the procedure used so far. Furthermore, if the result is confirmed, it inevitably implies an increase in the theoretical uncertainty in the determination of the axial charge, which must be more accurately estimated.

First, we test the sensitivity to the specific functional form eq. (24) of the parton distributions. To this purpose, we change the parameterization (24) by replacing the last factor with  $(1 + b_f\sqrt{x} + a_fx)$ , and then repeating the fit with various choices for the new parameters  $b_f$ . In particular, we fix  $b_q = b_g$  and then we vary  $-5 \leq b_q, b_{\text{NS}} \leq 5$ . No significant variation in the results or the quality of the global fit is found, indicating that the fit is stable. The results for extreme values of  $b_{\text{NS}}$  while  $b_q = b_g = 0$  are shown in table 2; variations of  $b_q, b_g$  produce even smaller effects.

Other sources of uncertainty related to the fitting procedure are due to the fact that the structure function is not measured over the full range of values of  $x$ , and is only sampled at a finite number of points. The former uncertainty comes from the extrapolations to small and large  $x$ , and is thus already included through the propagated errors in the six parameters  $\alpha_f$  and  $\beta_f$ . It is interesting to note that if we were to assume that the initial nonsinglet quark distribution was flat at small  $x$ , i.e.  $\alpha_{\text{NS}} = 0$ ,  $\Gamma_1$  would scarcely be altered, even though  $\eta_q$  and  $\eta_g$  both fall substantially (see table 2). The latter effect, however is due more to the deterioration in the quality of the fit at intermediate  $x$  than to a large change in the small  $x$  contribution. The other uncertainty is related to the fact that we determine the first moments of  $g_1$  and the parton distributions by integrating the respective best-fit forms. This is to be contrasted with the procedure followed by experimental collaborations, which instead determine the first moment of  $g_1$  by summing the data over the experimental bins; evolution effects could then be included as corrections to each bin separately. Such a procedure is however problematic because evolution effects are actually rather large in many of the bins, and furthermore the value of  $g_1(x_0, Q_0^2)$  is determined (nonlinearly) by the measurements at all  $x > x_0$  and  $Q^2 < Q_0^2$  so it is not possible to disentangle truly independent corrections to individual data points. Thus a simple sum over bins ignores the constraints imposed by perturbative evolution on the shape of  $g_1$  in the  $(x, Q^2)$  plane and gives undue weight to particular data points. The integration of fitted distributions has nevertheless an inevitable sampling uncertainty. To estimate this we have computed the difference between the experimental value of  $g_1$  in each bin and our best-fit  $g_1(x_b, Q_b^2)$ ,

where  $(x_b, Q_b^2)$  are the central values of  $x$  and  $Q^2$  for each  $x$  bin, and have then computed the first moment  $\Delta$  of this difference over the measured region by multiplying it by the bin width and summing over bins. We find  $\Delta^p(\text{SMC}) = -0.0032$ ,  $\Delta^p(\text{E143}) = 0.0007$ ,  $\Delta^d(\text{SMC}) = -0.0045$ ,  $\Delta^d(\text{E143}) = 0.0010$  for the four experiments, showing that this correction is indeed small and does not lead to a systematic bias. Combining these results we obtain an estimate for the overall statistical uncertainty due to the choice of the fitting procedure, to be added to that of the fit itself (see table 3).

We now turn to the various sources of systematic theoretical uncertainty. All the corresponding results, along with the  $\chi^2$  of the various fits, are summarized in table 2. First, we consider the possibility of SU(2) or SU(3) violation. The former will in general induce current mixing effects: for instance, in the presence of isospin violation, the proton and deuteron matrix element of the isosinglet current may be unequal to each other. However, due to the expected smallness of isospin violation, this effect is negligible compared to the error on the values of  $g_A$  and  $a_8$  induced by SU(2) and SU(3) violation in the quark distributions, which are then the dominant source of uncertainty. We estimate these by assuming a 2% uncertainty on  $g_A$  (of the same order of the accuracy to which isospin symmetry of unpolarized quark distributions may be established [32]) and a 30% uncertainty on  $a_8$  [33]. Notice that when these parameters are varied the size of the nonsinglet first moment of  $g_1$  varies; however, table 2 shows that the best-fit value of the singlet first moment and thus of  $a_0$  adjusts itself and remains surprisingly stable.

The uncertainty related to the value of  $\alpha_s$ , which is not negligible in a NLO computation, is simply estimated by repeating the fit when  $\alpha_s$  is varied in the range [34]  $\alpha_s(M_z) = 0.117 \pm 0.005$ . The position of the quark thresholds is varied from  $0.75m_q$  to  $2.5m_q$  (with  $m_c = 1.5$  GeV,  $m_b = 5$  GeV).

An important source of theoretical uncertainty is due to the lack of knowledge of higher order corrections, as reflected by the dependence of the results on factorization scale  $M^2$  and renormalization scale  $\mu^2$ . We estimate this by taking  $M^2 = k_1 Q^2$  and  $\mu^2 = k_2 Q^2$ , and varying  $0.5 \leq k_1, k_2 \leq 2$ . When the scales are varied the physical parameters turn out to have a stationary point within this range; the associated error is thus asymmetric, but rather large, consistent with the fact that evolution effects are important. The fluctuations found when varying the factorization scale are consistent with the spread of the results displayed in table 1 in various factorization schemes. We have also checked that including the known two and three loop corrections to the first moments of the coefficient functions produces similar variations.

The errors corresponding to all these sources, given by the maximal variation of the results as the parameters are varied in the respective ranges, are summarized in table 3. We have not included an error due to higher twist terms since we know of no reliable way of estimating it: experience with unpolarized data suggests that it is probably rather smaller than the error from higher order corrections.

In conclusion, the analysis of various sources of theoretical uncertainty confirms the stability of our determination of the first moment of  $g_1$  and the axial charge of the nucleon. Adding in quadrature the various sources of error, summarized in table 3, we get finally

$$\begin{aligned}
\Gamma_1^p(3 \text{ GeV}^2) &= 0.118 \pm 0.013 \text{ (exp.) }_{-0.006}^{+0.009} \text{ (th.)}, \\
\Gamma_1^d(3 \text{ GeV}^2) &= 0.024 \pm 0.013 \text{ (exp.) }_{-0.005}^{+0.011} \text{ (th.)}, \\
\Gamma_1^p(10 \text{ GeV}^2) &= 0.122 \pm 0.013 \text{ (exp.) }_{-0.005}^{+0.011} \text{ (th.)}, \\
\Gamma_1^d(10 \text{ GeV}^2) &= 0.025 \pm 0.013 \text{ (exp.) }_{-0.004}^{+0.012} \text{ (th.)}, \\
a_0(10 \text{ GeV}^2) &= 0.14 \pm 0.10 \text{ (exp.) }_{-0.05}^{+0.12} \text{ (th.)},
\end{aligned}
\tag{28}$$

The deuterium values refer to the structure function eq. (25); they must be multiplied by  $1 - 1.5\omega_D$  in order to compare with the results quoted by the experimental collaborations. Values of  $a_0$  at any other scale are obtained using NLO evolution [7]

$$a_0(Q^2) = \left[1 + \frac{2n_f}{\beta_0} \frac{\alpha_s}{\pi} + O(\alpha_s^2)\right] a_0(\infty), \quad (29)$$

which the expression (9)  $a_0$  satisfies by construction. The dominant source of theoretical uncertainty is that related to higher order corrections, i.e. to renormalization and factorization scale. The experimental uncertainty includes the various errors related to the fitting procedure (hence also the experimental systematics), and is still dominant. This is mainly due to the fact that the data allow us to only partly constrain the shape of the polarized gluon distribution, and thus the perturbative evolution of  $g_1$ .

It is interesting to compare the value of the axial charge eq. (28), obtained using eq. (9), with that obtained using eq. (11) with the coefficient functions expanded to NLO as in eq. (6):

$$a'_0(Q^2) \equiv [C_S(1, \alpha_s)]^{-1} \left( \frac{2}{\langle e^2 \rangle} \Gamma_1(Q^2) - C_{NS}(1, \alpha_s) \Delta q_{NS}(1, Q^2) \right). \quad (30)$$

If we could work to all orders  $a_0 = a'_0$ ; however, in a  $k$ -th order perturbative computation the two determinations differ by  $(k + 1)$ -th order corrections. Indeed, at NLO

$$a'_0(Q^2) - a_0(Q^2) = -2n_f \left( \frac{\alpha_s}{2\pi} \right)^2 \Delta g(1, Q^2) + O(\alpha_s^3). \quad (31)$$

This difference may be quite large if the gluon distribution is large: indeed, using eq. (30) we get  $a'_0(10 \text{ GeV}^2) = 0.09 \pm 0.15$  (stat.), which differs considerably from the central value eq. (28), though within the theoretical error. Notice that (31) is scale dependent: while it vanishes asymptotically, at low scales it is large enough that  $a'_0(Q^2)$  actually increases with  $Q^2$  below  $10 \text{ GeV}^2$  rather than decreasing as the axial charge should, according to eq. (29).

Finally, we can estimate the size of the quark and gluon distributions in the AB scheme:

$$\begin{aligned} \int_0^1 dx \Delta \Sigma(x) &= 0.5 \pm 0.1, \\ \int_0^1 dx \Delta g(x, 1 \text{ GeV}^2) &= 1.5 \pm 0.8, \end{aligned} \quad (32)$$

where all errors have been added in quadrature. The gluon distribution is rather large even at the quoted low scale (the corresponding value at  $10 \text{ GeV}^2$  is roughly twice as large) and even though the error is large, it differs significantly from zero. The value of the (scale independent) singlet quark distribution is in agreement within errors with the prediction of the Zweig rule, which would identify it with  $a_8$  eq. (27).

In summary, we have given a NLO determination of the main physical observables related to the polarized structure function  $g_1$ . Our main result is that the data already constrain the size of polarized parton distributions, and in particular require a rather large polarized gluon distribution. This in turn implies that perturbative evolution effects are

not negligible, and in fact substantially affect the extraction of the first moment of  $g_1$  from experimental data. Indeed, we find a value of the nonsinglet first moment which is significantly smaller than that obtained from a purely LO analysis. More importantly, we show that the error on the determination of the singlet axial charge of the nucleon is significantly larger than usually recognized, due essentially to the unknown effects of higher order perturbative corrections. The recent precise data on  $g_1$  are providing us with surprisingly accurate information on polarized parton distributions, but they also show that the theoretical and phenomenological interpretation of these data is significantly more subtle than previously expected.

**Acknowledgement:** We thank R. Mertig and W. van Neerven for providing details on their computations, P. Bosted, R. Erbacher, B. Frois and V. Hughes for information about the experimental data, and G. Altarelli, R.K. Ellis and G. Mallot for discussions.

## References

- [1] E143 Collaboration, K. Abe et al., *Phys. Rev. Lett.* **74** (1995) 346; SMC Collaboration, D. Adams et al., *Phys. Lett.* **B329** (1994) 399.
- [2] E143 Collaboration, K. Abe et al., *Phys. Rev. Lett.* **75** (1995) 25; SMC Collaboration, D. Adams et al., *Phys. Lett.* **B357** (1995) 248.
- [3] G. Altarelli and G. Ridolfi, *Nucl. Phys. B (Proc. Suppl.)* **39B** (1995) 106; S. Forte, hep-ph/9409416, in “Radiative Corrections: Status and Outlook”, B. F. L. Ward, ed. (World Scientific, Singapore, 1995); R. D. Ball, in the proceedings of the “International School on Nucleon Spin Structure”, Erice, August 1995 (to be published).
- [4] R. D. Ball, S. Forte and G. Ridolfi, *Nucl. Phys.* **B 444** (1995) 287.
- [5] R. Mertig and W. L. van Neerven, Leiden preprint INLO-PUB-6/95; Erratum, private communication (November 1995).
- [6] G. Altarelli and G. Parisi, *Nucl. Phys.* **B126** (1977) 298.
- [7] J. Kodaira et al., *Phys. Rev.* **D20** (1979) 627; *Nucl. Phys.* **B159** (1979) 99; J. Kodaira, *Nucl. Phys.* **B165** (1979) 129.
- [8] R. D. Carlitz, J. C. Collins and A. H. Mueller, *Phys. Lett.* **B214** (1988) 229.
- [9] G. Altarelli and B. Lampe, *Zeit. Phys.* **C47** (1990) 315.
- [10] W. Vogelsang, *Zeit. Phys.* **C50** (1991) 275.
- [11] G. Altarelli and G. G. Ross, *Phys. Lett.* **B212** (1988) 391.
- [12] S. Forte, *Nucl. Phys.* **B331** (1990) 1.
- [13] G.M. Shore and G. Veneziano, *Phys. Lett.* **B244** (1990) 75; *Nucl. Phys.* **B381** (1992) 23.
- [14] S. Adler and W. Bardeen, *Phys. Rev.* **182** (1969) 1517.
- [15] W. Furmanski and R. Petronzio, *Zeit. Phys.* **C11** (1982) 293.
- [16] E.B. Zijlstra and W.L. van Neerven, *Nucl. Phys.* **B417** (1994) 61.
- [17] S. A. Larin, *Phys. Lett.* **B334** (1994) 192.
- [18] M. Stratmann, A. Weber and W. Vogelsang, Dortmund preprint DO-TH 95/15, hep-ph/9509236
- [19] J. Bartels, B. I. Ermolaev and M. G. Ryshkin, DESY preprint 95-124.
- [20] R. D. Ball and S. Forte, *Phys. Lett.* **B351** (1995) 313.
- [21] M. A. Ahmed and G. G. Ross, *Phys. Lett.* **B56** (1975) 385; M. B. Einhorn and J. Soffer, *Nucl. Phys.* **B74** (1986) 714 ; A. Berera, *Phys. Lett.* **B293** (1992) 445.
- [22] T. Gehrmann and W. J. Stirling, Durham preprint DTP/95/78, hep-ph/9510243.
- [23] M. Glück et al., Dortmund preprint DO-TH 95-13 hep-ph/9508347.
- [24] L. W. Whitlow et al., *Phys. Lett.* **B250** (1990) 193.

- [25] NMC Collaboration, M. Arneodo et al. preprint CERN-PPE/95-138, [hep-ph/9509406](#).
- [26] L. L. Frankfurt and M. Strikman, *Nucl. Phys.* **A405** (1983) 557.
- [27] F. E. Close and R. G. Roberts, *Phys. Lett.* **B336** (1994) 257.
- [28] See S. J. Brodsky, M. Burkardt and I. Schmidt, *Nucl.Phys.* **B441** (1995) 197.
- [29] R. L. Heimann, *Nucl. Phys.* **B64** (1973) 429.
- [30] B.I. Ermolaev, S.I. Manayenkov and M.G. Ryskin, DESY preprint 95-017.
- [31] R. D. Ball and S. Forte, *Phys. Lett.* **B335** (1994) 77.
- [32] S. Forte, *Phys. Rev.* **D47** (1993) 1842.
- [33] B. Ehrnsperger and A. Schäfer, *Phys. Lett.* **B348** (1995) 619;  
J. Lichtenstadt and H. J. Lipkin, *Phys. Lett.* **B353** (1995) 119.
- [34] B. Webber, summary talk at the International Conference on High Energy Physics (ICHEP), Glasgow, Scotland, 1994, [hep-ph/9410268](#).

| parm.                | AB               | AR               | OS               |
|----------------------|------------------|------------------|------------------|
| $\eta_q$             | $0.48 \pm 0.09$  | $0.42 \pm 0.07$  | $0.35 \pm 0.04$  |
| $\eta_g$             | $1.52 \pm 0.74$  | $1.11 \pm 0.52$  | $0.99 \pm 0.23$  |
| $\alpha_{\text{NS}}$ | $-0.68 \pm 0.15$ | $-0.67 \pm 0.13$ | $-0.70 \pm 0.15$ |
| $\alpha_q$           | $0.41 \pm 0.38$  | $0.34 \pm 0.59$  | $0.97 \pm 0.65$  |
| $\alpha_g$           | $-0.47 \pm 0.30$ | $0.03 \pm 0.63$  | $0.35 \pm 0.67$  |
| $\beta_{\text{NS}}$  | $2.2 \pm 0.3$    | $1.3 \pm 0.3$    | $1.3 \pm 0.3$    |
| $\beta_q$            | $3.3 \pm 1.4$    | $2.1 \pm 1.0$    | $0.8 \pm 1.2$    |
| $\beta_g$            | $2.6 \pm 4.8$    | $7.0 \pm 8.3$    | 4 (fixed)        |
| $a_{\text{NS}}$      | $16 \pm 17$      | $8.6 \pm 8.2$    | $15 \pm 16$      |
| $a_q = a_g$          | $0.1 \pm 3.0$    | $0.9 \pm 4.4$    | $-1.25 \pm 0.09$ |
| $\chi^2$             | 62.6/63          | 61.0/63          | 61.8/64          |

Table 1: Best-fit values of the parameters eq. (24) and  $\chi^2$  for fits in the AB, AR and OS schemes; the errors shown are statistical only.

|                          | $\eta_q$        | $\eta_g$        | $\Gamma_1^p(10)$  | $\Gamma_1^d(10)$  | $a_0(10)$       | $\chi^2$ |
|--------------------------|-----------------|-----------------|-------------------|-------------------|-----------------|----------|
| as tab. 1                | $0.48 \pm 0.09$ | $1.52 \pm 0.74$ | $0.122 \pm 0.013$ | $0.025 \pm 0.013$ | $0.14 \pm 0.10$ | 62.6     |
| high $b_{\text{NS}}$     | $0.48 \pm 0.06$ | $1.43 \pm 0.48$ | $0.124 \pm 0.011$ | $0.027 \pm 0.011$ | $0.15 \pm 0.08$ | 63.2     |
| low $b_{\text{NS}}$      | $0.50 \pm 0.10$ | $1.55 \pm 0.81$ | $0.123 \pm 0.015$ | $0.027 \pm 0.015$ | $0.15 \pm 0.11$ | 64.3     |
| $\alpha_{\text{NS}} = 0$ | $0.37 \pm 0.09$ | $1.17 \pm 0.70$ | $0.120 \pm 0.010$ | $0.023 \pm 0.010$ | $0.11 \pm 0.08$ | 73.9     |
| high $g_A$               | $0.48 \pm 0.09$ | $1.54 \pm 0.74$ | $0.124 \pm 0.013$ | $0.025 \pm 0.013$ | $0.14 \pm 0.10$ | 62.5     |
| low $g_A$                | $0.48 \pm 0.09$ | $1.50 \pm 0.73$ | $0.120 \pm 0.012$ | $0.026 \pm 0.012$ | $0.14 \pm 0.10$ | 62.7     |
| high $a_8$               | $0.45 \pm 0.09$ | $1.58 \pm 0.74$ | $0.122 \pm 0.013$ | $0.026 \pm 0.013$ | $0.10 \pm 0.10$ | 62.7     |
| low $a_8$                | $0.51 \pm 0.09$ | $1.47 \pm 0.73$ | $0.122 \pm 0.012$ | $0.025 \pm 0.012$ | $0.18 \pm 0.10$ | 62.5     |
| high $\alpha_s$          | $0.51 \pm 0.08$ | $1.36 \pm 0.55$ | $0.118 \pm 0.013$ | $0.022 \pm 0.013$ | $0.12 \pm 0.10$ | 63.6     |
| low $\alpha_s$           | $0.47 \pm 0.09$ | $1.80 \pm 0.82$ | $0.124 \pm 0.011$ | $0.026 \pm 0.011$ | $0.14 \pm 0.09$ | 62.1     |
| high fact.               | $0.42 \pm 0.05$ | $1.17 \pm 0.45$ | $0.121 \pm 0.010$ | $0.023 \pm 0.010$ | $0.11 \pm 0.08$ | 61.1     |
| low fact.                | $0.41 \pm 0.07$ | $0.81 \pm 0.39$ | $0.133 \pm 0.007$ | $0.037 \pm 0.007$ | $0.25 \pm 0.06$ | 63.0     |
| high ren.                | $0.42 \pm 0.05$ | $1.31 \pm 0.57$ | $0.125 \pm 0.010$ | $0.028 \pm 0.010$ | $0.15 \pm 0.07$ | 61.4     |
| low ren.                 | $0.42 \pm 0.08$ | $0.92 \pm 0.59$ | $0.129 \pm 0.016$ | $0.033 \pm 0.016$ | $0.20 \pm 0.13$ | 62.3     |
| high thr.                | $0.57 \pm 0.06$ | $1.69 \pm 0.33$ | $0.121 \pm 0.006$ | $0.024 \pm 0.006$ | $0.13 \pm 0.06$ | 62.5     |
| low thr.                 | $0.46 \pm 0.07$ | $1.54 \pm 0.67$ | $0.121 \pm 0.012$ | $0.025 \pm 0.012$ | $0.13 \pm 0.10$ | 62.0     |

Table 2: Values of the parameters  $\eta_q$  and  $\eta_g$ , the first moment of  $g_1$  eq. (8), the axial charge eq. (9) and  $\chi^2$  (64 degrees of freedom for the entry  $\alpha_{\text{NS}} = 0$  and 63 d.f. for all other entries), all calculated in AB scheme, for the various fits discussed in the text.

| source               | $\Delta\Gamma_1^p(10)$ | $\Delta\Gamma_1^d(10)$ | $\Delta a_0(10)$ |
|----------------------|------------------------|------------------------|------------------|
| fit (statistical)    | $\pm 0.013$            | $\pm 0.013$            | $\pm 0.10$       |
| fitting procedure    | $\pm 0.003$            | $\pm 0.003$            | $\pm 0.03$       |
| SU(2) violation      | $\pm 0.002$            | $\pm 0.000$            | $\pm 0.00$       |
| SU(3) violation      | $\pm 0.000$            | $\pm 0.000$            | $\pm 0.04$       |
| value of $\alpha_s$  | +0.002<br>-0.004       | +0.001<br>-0.003       | +0.00<br>-0.02   |
| thresholds           | $\pm 0.001$            | $\pm 0.001$            | $\pm 0.01$       |
| higher order corrns. | +0.011<br>-0.002       | +0.012<br>-0.003       | +0.11<br>-0.03   |

Table 3: Errors in the determination of  $\Gamma_1$  and  $a_0$ .

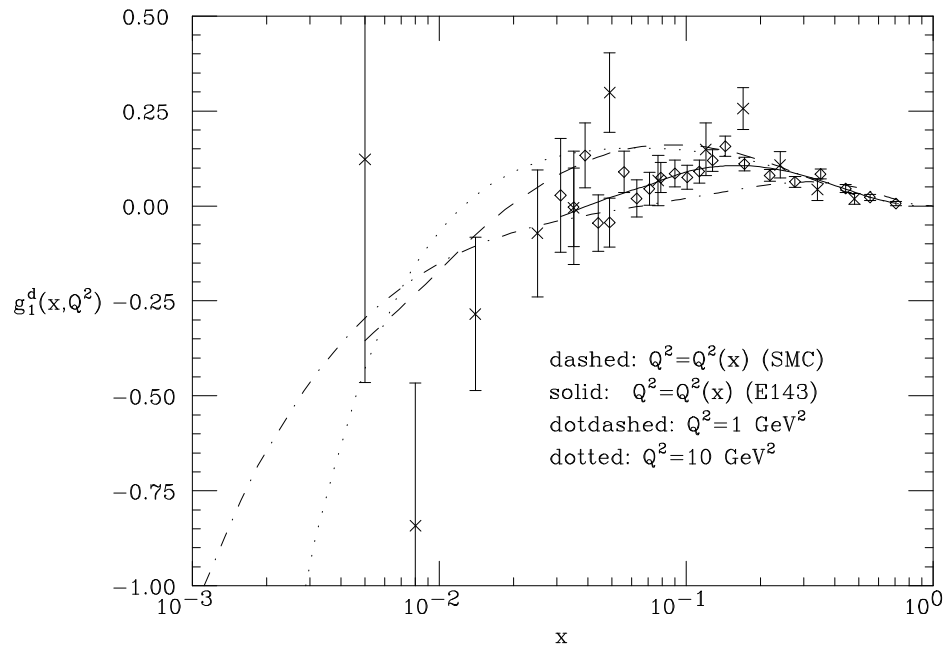
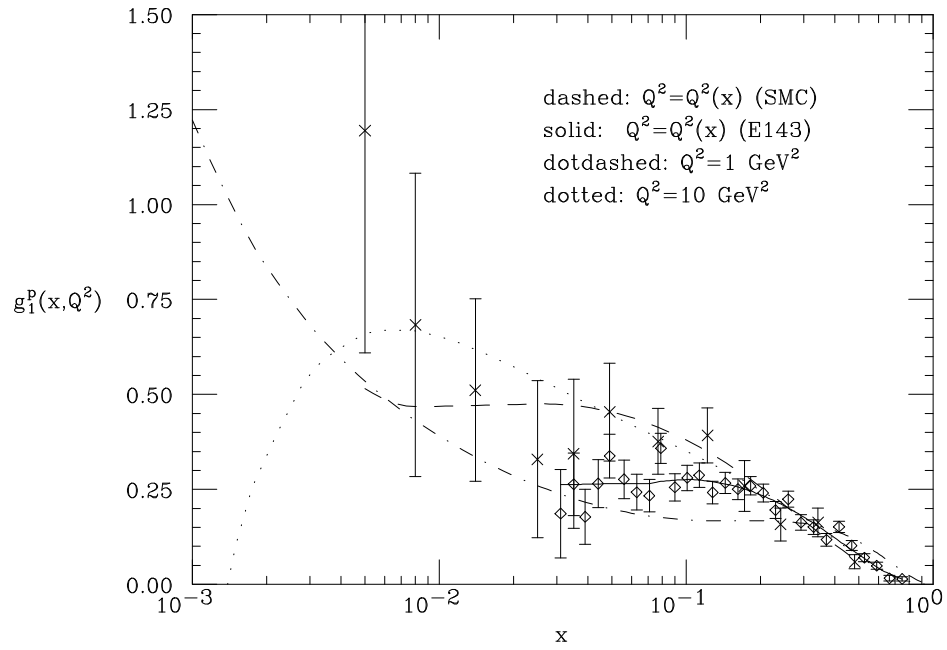


Fig. 1i

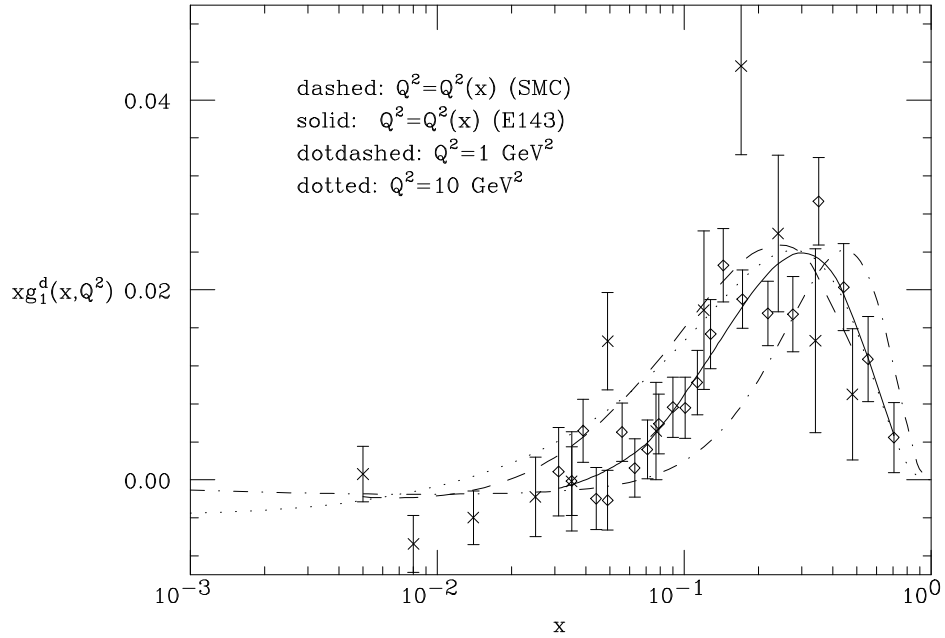
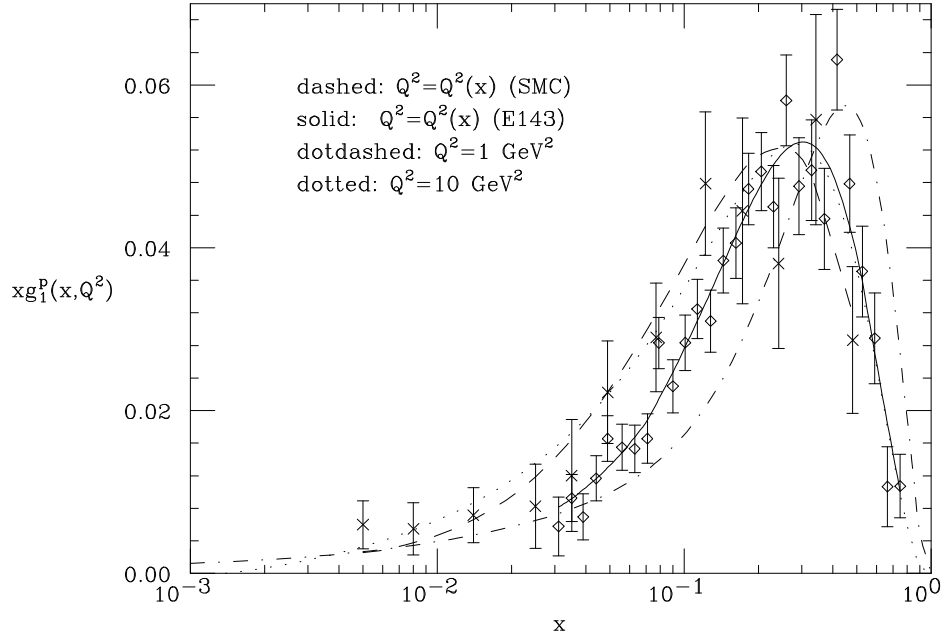


Fig. 1ii

Plots of  $g_1(x)$  (i) and  $xg_1(x)$  (ii) compared to the SMC (crosses) and E143 (diamonds) experimental data for (a) proton and (b) deuteron. The curves correspond to a NLO computation in the AB scheme with the initial parton distributions eq. (24) and the values of the parameters given in table 1.